Failure modes and optimal performance of a generic synchronizer

N.B. When citing this work, cite the original published paper.

(article starts on next page)

Failure modes and optimal performance of a generic synchronizer

Muhammad Irfan, Viktor Berbyuk and Håkan Johansson

Mechanics and Maritime Sciences, Chalmers University of Technology, Göteborg, Sweden
{i*rfan.muhammad, viktor.berbyuk, hakan.johansson*}@*chalmers.se*

ABSTRACT *The gear shifting mechanism is a crucial part of the gearbox which transmits the torque from engine to wheels with different transmission ratio. For smooth and comfortable gear changing the gear shifting mechanism is still a challenge for the engineers to adapt the different driving situations. In case of heavy vehicles particularly under certain circumstances optimized performance by avoiding failure modes of the gear shifting mechanism is also a challenge. In this paper failure modes and optimized values of the system parameters are identified to contribute for this challenge. A model of the gear shifting mechanism is developed in GT-Suite software. Failure modes are identified via sensitivity analysis. Four system response characteristics are plotted against the time and used to identify the failure modes. Optimization routine of the GT-Suite is applied on the model by taking seven parameters into account as independent variables and synchronization time as an objective function. Percentage changes of the variables from their initial values are calculated and analyzed. Finding of optimal values of parameters of the gear shifting mechanism is valuable contribution to design reliable and efficient transmission system for automotive industry especially for heavy vehicles.*

1 Introduction

Automotive industry has been working to improve the gear shifting technology especially for heavy vehicles. The traditional bulk ring synchronizer is still an important design, Figure 1, and is subjected to several studies. Key components of the bulk ring design are the friction cones, blocking chamfer and engaging teeth, and detailed studies of these have been carried out. For instance, Häggström et al. presented thermomechanical model of the friction lining using the finite element tool Abaqus/Standard [1]. In [2] Häggström et al. predicted failure of the molybdenum coated gearbox synchronizers through the thermomechanical load in terms of kinetic energy, synchronization power, focal and average surface temperature. Szöky et al. solved the problem of scratching on dog teeth during the gear shifting by decreasing sleeve chamfer, gear piece angle and tip radius. Further, cold chamfer tests and the sleeve chamfer durability tests were conducted with satisfying results [3]. Bóka et al. built the mechanical model to describe the uncertainty of clashing and probability of successful engagement [4]. Lovas incorporated mathematical models of the gear shifting process in a numerical simulation software to describe the gear shifting process with the concern of manufacturing as well. In addition to this he explained operational problems, for example double bump, stick slip phenomenon, etc with the suggestions of improvements [5].

To simulate the complete synchronization process consisting of several sub-phases mathematical model of the generic gear shifting mechanism was developed in [6, 7] based on constrained Lagrangian formalism. The mathematical model was made possible to allow for simple change of a friction model, gearbox type, actuator model, etc. The model was used for sensitivity analysis [8]. The gear shifting process is optimized by implementing Matlab optimization routine with the genetic algorithm [9]. In order to better describe and identify different types of failure modes, and to optimize the performance, which is the subject of the present study, a gear shifting mechanism model is developed in GT-Suite software.

2 Modelling of the gear shifting mechanism

GT-Suite software is used to develop a model of the gear shifting mechanism with five degrees of freedom. The generic synchronizer as shown in Figure 1 consists of three rigid bodies: engaging sleeve, synchronizer ring and gearwheel. The engaging sleeve and the gearwheel have different rotational speeds and need to engage with each other by engaging teeth to shift the gear at transmission. The synchronizer ring plays a role to decrease the speed difference by blocking the sleeve for a while and afterwards allows both rigid bodies to engage with each other. Values of parameters of the generic synchronizer which are common in [7, 8] and this study are given in Table 1.
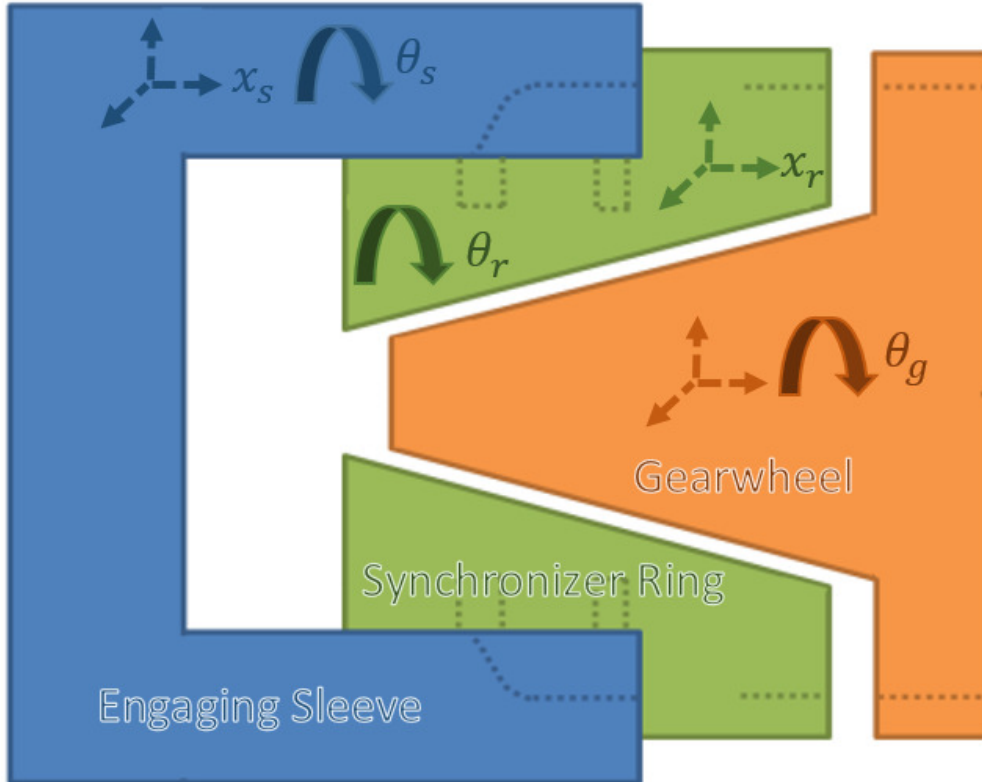

Figure 1: The generic synchronizer [6].

Variable	Name	Variable	Name
$m_s = 1.5$ kg	Sleeve mass	$m_r = 0.5$ kg	Ring mass
$I_g = 0.2$ kgm^2	Gear moment of inertia	$I_s = 0.01$ kgm^2	Sleeve moment of inertia
$I_r = 0.004$ kgm^2	Ring moment of inertia	$r_\beta = 0.07$ m	Chamfers mean radius
$r_\alpha = 0.1$ m	Cones mean radius	$d_\alpha = 2$ mm	Cones Initial clearance
$b = 5$ mm	Cones contact length	$B_{ang} = 5^o$	Angle clearance
$\beta = 60^o$	Chamfer angle	$\mu_\alpha = 0.17$	Cones friction coefficient
$\alpha = 7^o$	Cone angle	$\mu_\beta = 0.09$	Blocker friction coefficient
$C_{r\alpha} = 0.002$	Ring sliding friction	$C_{s\alpha} = 0.02$	Sleeve sliding friction
$\omega_{s_o} = 1000$ rpm	Sleeve rotational speed	$\omega_{g_o} = 700$ rpm	Initial gear rotational speed
$F_{shf} = 1000$ N			

Table 1: Values of the generic synchronizers parameters used in [7].

The vector of generalized coordinates of the synchronizer system is given below

$$\mathbf{q} = \left[x_s, \theta_s, x_r, \theta_r, \theta_g\right]^T \tag{1}$$

where θ_s, θ_r and θ_g are angular coordinates of sleeve, ring and gearwheel, respectively; x_s and x_r are translational coordinates of the sleeve and ring, respectively.

Multibody systems can be modelled on GT-Suite software with their particular features which can be active during their practical functioning. GT-Suite model of the gear shifting mechanism consists of three rigid bodies: sleeve, ring and gear as shown in Figure 2. A rigid body has six degrees of freedom in space but to develop the synchronizer some of degrees of freedom of the rigid bodies are freezed. The synchronizer has five degrees of freedom. The sleeve and the ring can translate axially and rotate about axial direction. The gear can only rotate about axial direction. In this study of model developed in the GT-Suite software the gear shifting process is divided into three phases; presynchronization, main synchronization and engagement. The phase from start to the moment when cones come in contact is called presynchronization. The phase during which the cones slide over each other with pressure to decrease the speed difference is called main synchronization. The third phase starts when speed difference becomes zero and ends when the engagement of teeth is done to finish the gear shifting process. At neutral position the sleeve and the gear have different rotational speeds and to shift the gear the sleeve and the gear must engage with each other. So it is necessary to decrease the speed difference for successful engagement of the teeth. Therefore the three rigid bodies are connected with each other in such a way to shift the gear without clashing. The sleeve and the ring are connected with spring and blocking teeth. The ring and the gear are connected with cones. The gear and the sleeve are connected with engaging teeth. Further four options ring-strut-contact, passing-of-speed, constant speed and force are selected from graphical user interface of the GT-Suite software to model a simple but complete gear shifting process. The gear shifting process starts when the shift force is applied. At start of the process the sleeve moves axially. The option of ring-strut-contact creates an initial angular gap between the sleeve and the ring which will appear in blocking teeth. When the sleeve starts to translate axially, the spring slows down the sleeve translational movement to bring the blocking teeth at indexing position. When the blocking teeth come in contact, the ring also starts to translate axially with the sleeve until the cones come in contact. Meanwhile the ring rotates with the sleeve rotational speed because of attribute of the passing-of-speed of the GT-Suite software. After the cones come in contact, the sleeve stops its translational movement. The speed difference decreases between the sleeve and the gear because of the cones sliding under pressure. Only rotational speed of the gear varies while rotational speed of the sleeve remains constant even throughout the gear shifting process because of attribute of constant-speed of the software. When the speed difference decreases to zero, the blocking teeth releases the sleeves blockage and the sleeve moves forward to get engagement with the gear. At end of the process teeth of the sleeve and the gear come in full contact implemented by the engaging-teeth attribute as shown in Figure 2.
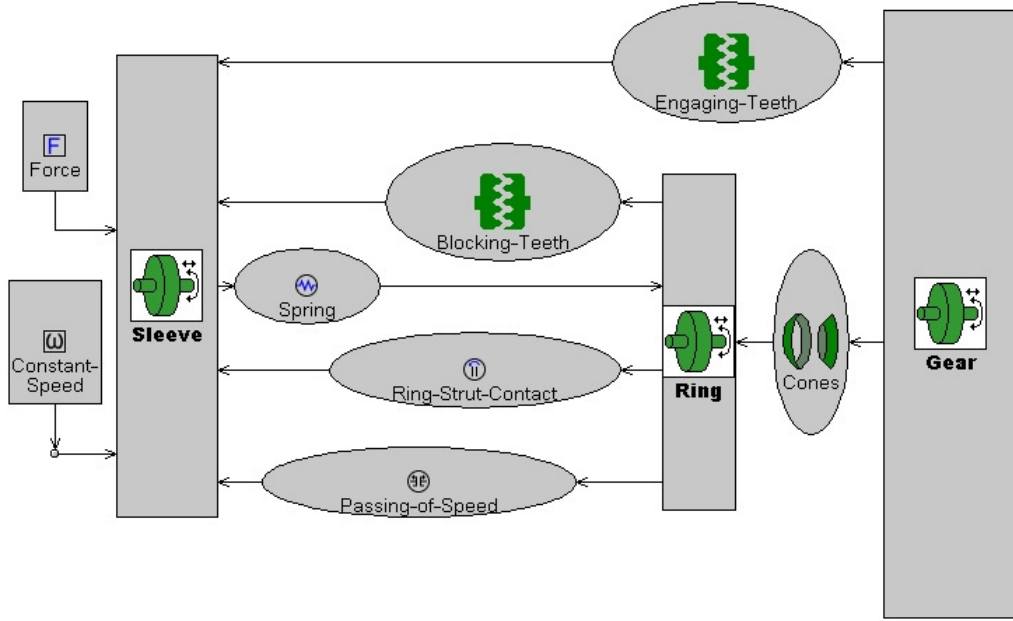
Figure 2: GT-Suite model of simplified gear shifting mechanism.

A model of the gear shifting mechanism has developed in GT-Suite software. Seven parameters of the generic synchronizer are taken as input to the gear shifting mechanism and categorized as the control design parameter and the structural design parameters which are given below

$$\text{Control design parameter} = [\text{Shift force}] = F_{shf}$$

$$\text{Structural design parameters} = \begin{bmatrix} \text{Blocker angle} \\ \text{Indexing angle} \\ \text{Cone angle} \\ \text{Cone coefficient of friction} \\ \text{Cone radius} \\ \text{Spring force} \end{bmatrix} = \begin{bmatrix} \beta \\ \delta \\ \alpha \\ \mu_\alpha \\ r_\alpha \\ F_{spr} \end{bmatrix} \quad (2)$$

The gear shifting process is monitored by the control design parameter F_{shf}, gear shifting time t and the following vector

$$\begin{bmatrix} \text{Sleeve rotational speed} \\ \text{Gear rotational speed} \\ \text{Sleeve axial displacement} \end{bmatrix} = \begin{bmatrix} \omega_s \\ \omega_g \\ d_\alpha \end{bmatrix} \quad (3)$$

The gear shifting process modelled on GT-Suite software is sum up in three main phases; pre-synchronization (phase 1), main synchronization (phase 2) and engagement (phase 3). So, the constraints will be imposed upon motion of the synchronizer modelled in GT-Suite software. These constraints are presented in Table 2.

Phase	Constraints	Phase	Constraint
1	$\begin{bmatrix} x_s - x_r - x_{s1} \\ \theta_s - \theta_r - \delta \end{bmatrix} = \mathbf{0}$	3	$\begin{bmatrix} x_s - x_r - x_{s12} \\ \theta_s - \theta_r - \theta_{rs} \\ \theta_s - \theta_g - \theta_{sg} \end{bmatrix} = \mathbf{0}$
2	$\begin{bmatrix} x_s - x_r - x_{s12} \\ \theta_s - \theta_r - \theta_{rs} \end{bmatrix} = \mathbf{0}$		

Table 2: Internal constraints during phases of the synchronization.

During phase 1 the ring moves axially from its initial position and covers a displacement of $\pm x_{r_{tol}}$ while the sleeve moves axially and covers a displacement of $x_{s1} + x_{s_{tol}}$ as shown in eq. (4). The variable $x_{s_{tol}}$ has a maximum value of 5 mm and minimum value of 0 mm. The variable $x_{r_{tol}}$ varies between 0 mm and 1.5 mm. During phase 2 the ring and the sleeve stay at their positions of x_{r2} and x_{s2} respectively. In phase 3 the sleeve moves axially from x_{s2} to x_{s3} while the ring return to its initial positon at x_{r1} from x_{r2}. But where the phase 1 ends at value of $(x_{s1} + x_{s_{tol}})$ the ring will not proceed further axially during phase 2 and $\pm x_{r_{tol}}$ will be called x_{r2}. The variable $(x_{s1} + x_{s_{tol}})$ will be called x_{s2} during phase 2. Values of $x_{r_{tol}}$ and $x_{s_{tol}}$ depend upon stiffness of the system.

$$\begin{cases} x_{r1} \leq x_r \leq \pm x_{r_{tol}} & 0 \leq x_s \leq x_{s1} + x_{s_{tol}} & Phase\ 1 \\ x_r = x_{r2} & x_s = x_{s2} & Phase\ 2 \\ x_{r2} \geq x_r \geq x_{r1} & x_{s2} \leq x_s \leq x_{s3} & Phase\ 3 \end{cases} \tag{4}$$

The followings are assumed

$$0 \leq x_{r_{tol}} \leq 1.5,\ 0 \leq x_{s_{tol}} \leq 5,\ x_{r1} = 15\ mm,\ x_{s1} = 9\ mm,\ x_{s3} = 20\ mm,\ x_{r3} = x_{r2}$$
$$x_{s2} = x_{s1} \pm x_{s_{tol}}\ and\ x_{r2} = x_{r1} \pm x_{r_{tol}}\ at\ end\ of\ phase\ 1,\ x_{s12} = (x_{s1} \pm x_{s_{tol}}) - (\pm x_{r_{tol}})$$

In phase 1 the ring must get its indexing position by covering a rotational displacement of δ before blocking teeth of the sleeve come in contact with blocking teeth of the ring and the blocking teeth come in contact when the sleeve covers x_{s1} axial displacement. After the blocking teeth contact the ring and the sleeve rotate together till end of the synchronization process as shown in eq. (5).

$$\begin{cases} 0 \leq \theta_r \leq \delta & 0 \leq x_s \leq x_{s1} & Phase\ 1 \\ \theta_r = \theta_s - \delta & x_{s1} \leq x_s \leq x_{s1} + x_{s_{tol}} & Phase\ 1 \\ \theta_r = \theta_s - \delta & x_s = x_{s2} & Phase\ 2 \\ \theta_r = \theta_s - \delta & x_{s2} \leq x_s \leq x_{s3} & Phase\ 3 \\ \theta_g = \theta_s - \theta_{sg} & x_{s2} \leq x_s \leq x_{s3} & Phase\ 3 \end{cases} \tag{5}$$

$$\theta_{rs} = \theta_s - \theta_r\ at\ end\ of\ phase\ 1,\ \theta_{sg} = \theta_s - \theta_g\ at\ end\ of\ phase\ 2$$

Let's the mechanism modelled on GT-Suite software has given initial state of the general coordinates (1) and nominal values of the structural design parameters $[\beta_o, \delta_o, \alpha_o, \mu_{\alpha_o}, r_{\alpha_o}, F_{spr_o}]^T$ and the vector $[\omega_{s_o}, \omega_{g_o}, d_{\alpha_o}]^T$ as follows

$$\begin{bmatrix} \beta_o \\ \delta_o \\ \alpha_o \\ \mu_{\alpha_o} \\ r_{\alpha_o} \\ F_{spr_o} \end{bmatrix} = \begin{bmatrix} 60^o \\ 4^o \\ 7^o \\ 0.17 \\ 100 \ mm \\ 100 \ N \end{bmatrix}, \ \mathbf{q} = \begin{bmatrix} \theta_{s_o} \\ \theta_{g_o} \\ x_{s_o} \\ x_r \\ \theta_r \end{bmatrix} = \begin{bmatrix} 0^o \\ 0^o \\ 0.2 \ mm \\ 15 \ mm \\ 0^o \end{bmatrix}, \ \dot{\mathbf{q}} = \begin{bmatrix} \dot{\theta}_{s_o} \\ \dot{\theta}_{g_o} \\ \dot{x}_{s_o} \\ \dot{x}_{r_o} \\ \dot{\theta}_{r_o} \end{bmatrix} = \begin{bmatrix} \omega_{s_o} \\ \omega_{g_o} \\ \dot{x}_{s_o} \\ \dot{x}_{r_o} \\ \dot{\theta}_{r_o} \end{bmatrix} = \begin{bmatrix} 1000 \ rpm \\ 700 \ rpm \\ 0 \\ 0 \\ 0 \end{bmatrix} \tag{6}$$

The mechanism has a constraint $\omega_s = constant$ which holds till end of the gear shifting process.

The shift force $F_{shf} = 1000 \ N$ is applied on the mechanism and resulted performance of the mechanism described by the synchronizer performance diagram is shown in Figure 3 with axial movement of the sleeve, rotational speed of the gear and the sleeve, the shift force and the synchronization time, t_{synch}.

Here the shift force and time history of the sleeve and the gear are plotted. The shift force of 1000 N is applied from point **k** to point **l**. The sleeve moves axially from point **a** to point **b** and comes in contact with spring, blocking teeth and the ring. At start of the process cones come in contact but without having a pressure. At point **b** the cones get pressure because of the applied shift force and hold the sleeve until the speed difference decreases to zero as shown from point **b** to point **c**. From point **c** the sleeve moves axially again and comes in contact with engaging teeth of the gear at point **d**. From point **d** to point **e** the gear and the sleeve engage completely with each other through the engaging teeth. The gear does not gain a sufficient increment in rotational speed from point **f** to point **g** because the cones are sliding over each other without having a pressure but afterwards when the cones get pressure by the shift force the gear gains rotational speed sharply and at point **h** the gear reaches at the rotational speed of the sleeve. As shown from point **m** to point **n** the sleeve rotates with constant speed. The synchronization time, t_{synch} of the gear shifting process is 0.118 sec.
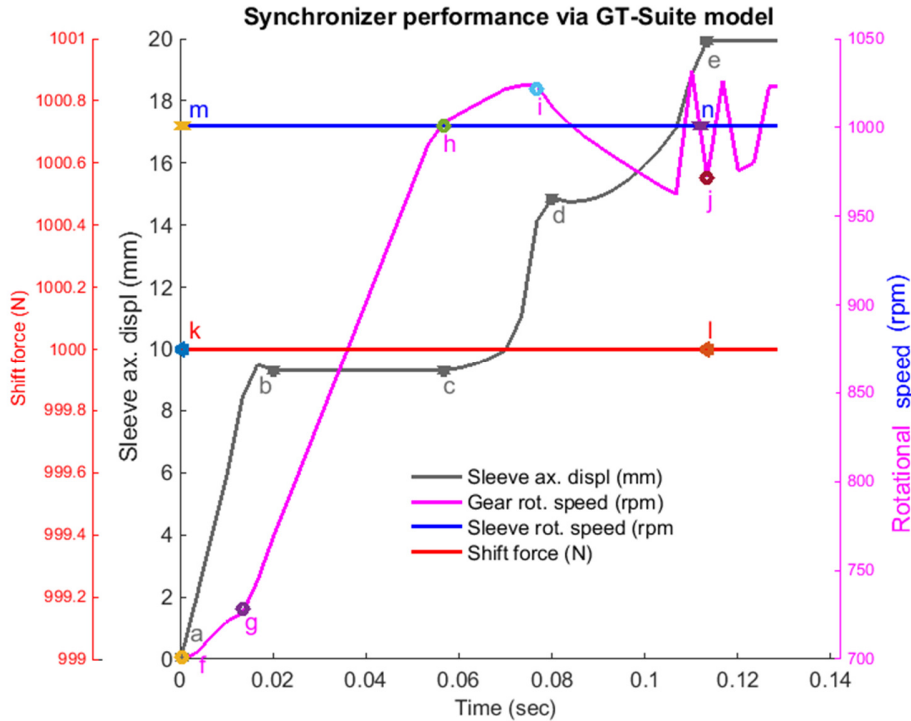

Figure 3: Synchronizer performance diagram by GT-Suite model.

3 Prediction of failure modes via sensitivity analysis

For performance improvement of the synchronizer it is important to know the reasons for failure. The mechanism failures by clashing of the engaging teeth, complete blockage of the sleeve and undesirable longer synchronization time are studied. The GT-Suite model is simulated by varying values of one of the parameters in a reasonable bounds [7] while rest of the parameters have constant values. A constant force is applied for a single simulation on GT-Suite software. In this way those values of the parameters one by one are identified at which the synchronizer causes failures.

3.1 The sensitivity analysis of the gear shifting mechanism

Failure of the gear shifting mechanism can be identified by different kind of techniques for example by parameters sensitivity analysis, sensors, condition monitoring, etc. In this study sensitivity analysis is chosen where values of the synchronizers parameters are varied to observe the effect upon performance of the synchronizer.

The gear shifting process is monitored based on system response characteristics by varying variables of the synchronizer including structural design parameters and control design parameters. Sleeve axial displacement, ring axial displacement, speed difference between the sleeve and the gear and relative rotation of the blocking teeth are taken as system response characteristics. Shift force as a control design parameter and spring force, blocking teeth angle, indexing angle, cone angle, cone radius and cone coefficient of friction are taken as structural design parameters. Reasonable bounds of values of the control design and structural design parameters are chosen as considered in [7]. Particular value of each parameter is identified at which the synchronizer fails to perform. In GT-Suite model the control design and structural design parameters are considered as independent parameters and synchronization time as dependent parameter. The synchronization time decreases or increases with variations of values of the parameters. It is understood that practically it is not possible to achieve the ideal case. So, in one case beyond the possible highest or lowest synchronization time the mechanism fails to perform. In second case if the synchronizer perform optimally at one end of the values bound, at other end of the values bound the synchronizer perform poorly or probably fails to perform. That particular value for each independent parameter is found through sensitivity analysis as shown in Figure 4-9.

3.2 Identification of failure modes

The control design parameter and the structural design parameters are varied from lowest to highest values of elements of column vectors one by one as shown in (7)

$$
F_{shf} = \begin{bmatrix} 600 \\ 1000 \\ 2000 \\ 2100 \end{bmatrix}, \quad
\beta = \begin{bmatrix} 40^o \\ 60^o \\ 65^o \\ 70^o \\ 75^o \\ 80^o \\ 85^o \end{bmatrix}, \quad
\delta = \begin{bmatrix} 2^o \\ 4^o \\ 8^o \\ 12^o \end{bmatrix}, \quad
\alpha = \begin{bmatrix} 05^o \\ 07^o \\ 09^o \\ 11^o \\ 17^o \\ 19^o \\ 21^o \end{bmatrix}, \quad
\mu_\alpha = \begin{bmatrix} 0.12 \\ 0.17 \\ . \\ . \\ . \\ 0.72 \\ 0.77 \end{bmatrix}, \quad
r_\alpha = \begin{bmatrix} 60 \\ 70 \\ 80 \\ 90 \\ 100 \\ 110 \\ 120 \\ 130 \\ 140 \end{bmatrix}, \quad
F_{spr} = \begin{bmatrix} 400 \\ 600 \\ 800 \\ 1000 \\ 12000 \\ 14000 \end{bmatrix} \tag{7}
$$

Vector of the parameters $[\omega_s, \omega_g, d_\alpha]^T$ and the synchronization time t_{synch} are obtained for each varying value of each parameter.

System response characteristics as shown below are selected to be used for synchronization failure modes prediction

$$\text{System response characteristics} = \begin{bmatrix} \text{Sleeve axial displacement} \\ \text{Ring axial displacement} \\ \text{Speed difference} \\ \text{Relative rotation of blocking teeth} \end{bmatrix} = \begin{bmatrix} x_s \\ x_r \\ \Delta\omega_{s-g} \\ \Delta\theta_{s-r} \end{bmatrix} \qquad (8)$$

Failure modes as defined in section 3 are described mathematically here

$$Failure\ modes = \begin{bmatrix} \text{mode 1} \\ \text{mode 2} \\ \text{mode 3} \end{bmatrix} = \begin{bmatrix} clashing \\ blocking \\ longer\ t_{synch} \end{bmatrix} \qquad (9)$$

$$\begin{bmatrix} clashing \\ clashing \\ blocking \\ longer\ t_{synch} \end{bmatrix} = \begin{cases} t \le t_{clash} & x_s = d_{rg}, & Phase\ 2 \\ \theta_{g_s} \ge \theta_{clash} & d_{sr} \le x_s \ge d_{sg}, & Phase\ 3 \\ t_{synch} = inf & x_s = d_{rg}, & Phase\ 2 \\ t_{synch} > t_{accept} & d_{sr} \le x_s \ge d_{sg}, & Phase\ 3 \end{cases} \qquad (10)$$

Values of θ_{clash}, t_{accept} and t_{clash} depend upon the practical application and type of the gear shifting mechanism but reasonable values as shown in (11) are chosen for study.

$$\theta_{clash} = 100\ rpm,\ t_{accept} = 0.2\ sec,\ t_{clash} = 0.05\ sec \qquad (11)$$

By monitoring the system response characteristics $(x_{sl}, x_{rg}, \Delta\omega_{s-g}, \Delta\theta_{s-r})$ and checking with the failure modes conditions, values of the parameters are identified at which the mechanism fails to perform.

System response characteristics are plotted against the time at different values of the control design and structural design parameters as shown in Figure 4-9. It is studied that variation of the control design and structural design parameters either decrease or increase the synchronization time, t_{synch}. It is also observed that how the system response characteristics vary with the time during synchronization process which helps to identify the failure modes.

Synchronization time, t_{synch} for gear shifting process decreases with increasing shift force as shown by the sleeve axial displacement in Figure 4 (a). Ultimately because the sleeve covers the displacement quickly, the synchronizer fails to perform. The system response characteristics against the time are plotted at 600 N, 1000 N, 2000 N, 2500 N, 3000 N and 4000 N shift forces as shown in Figure 4. The sleeve axial displacements before 3000 N shift force shows feasible gear shifting process. But at 3000 N and 4000 N shift forces the process fails because the sleeve does not stay for a sufficient time during the cones sliding and approaches the engagement teeth which produce clashing. Shorter stay of the sleeve is shown in Figure 4 (a). Equal and higher than 3000 N shift force produces failure of the gear shifting process or unfeasible synchronization. Similarly unsmooth behaviors in case of ring axial displacement, speed difference and relative rotation of blocking teeth are observed as shown in Figure 4 (b-d).

Synchronization time increases with increasing blocker angle as shown in Figure 5 (a). Blockage of the sleeve for longer time causes the longer synchronization time. At 80° blocker angle the sleeve does not move further from blocking positon as shown in the Figure 5 (a) which indicates failure of the process. From the ring axial displacement and the speed difference it is hard to predict the failure mode with varying blocker angle.

Synchronization time does not change significantly by increasing indexing angle but increment in indexing angle can cause the failure mode. In Figure 6 (a) shows that the sleeve stops at 7° indexing angle which causes failure in gear shifting process. This failure is categorize as blockage. Similarly the mechanism behaves unexpectedly at 7° indexing angle as shown in Figure 6 (b), (d).

From the implemented GT-Suite model in this study it is hard to predict the failure mode with increasing the cone angle although Figure 7 shows that the synchronization time increases with increasing the cone angle. The wedging condition of the sliding cones is not applied in this model. But in practical application the wedging condition must be satisfied otherwise the cones can be welded over each other during sliding. If the failure mode is defined in terms of undesirable longer synchronization time, failure mode can be predictable with knowledge of value of the undesirable synchronization time.
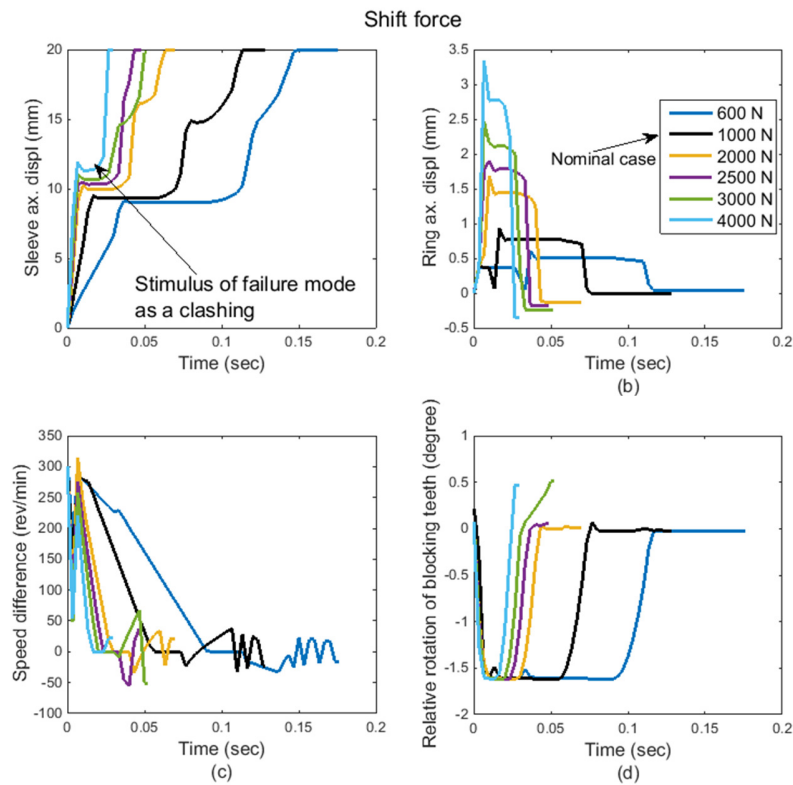

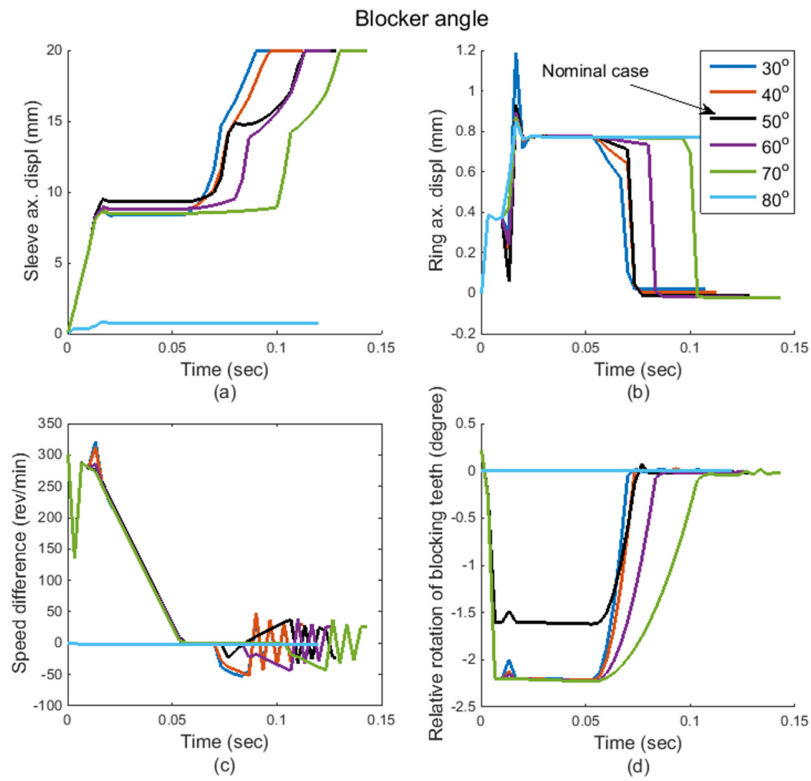Figure 4: Synchronization failure modes prediction by varying shift force.

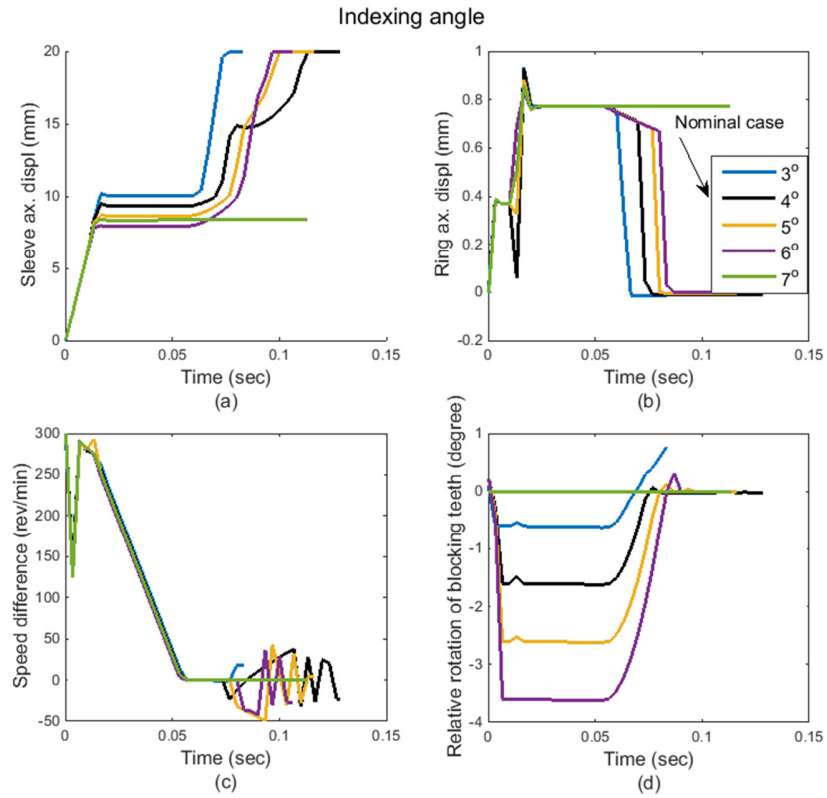Figure 5: Performance monitoring by varying blocker angle.

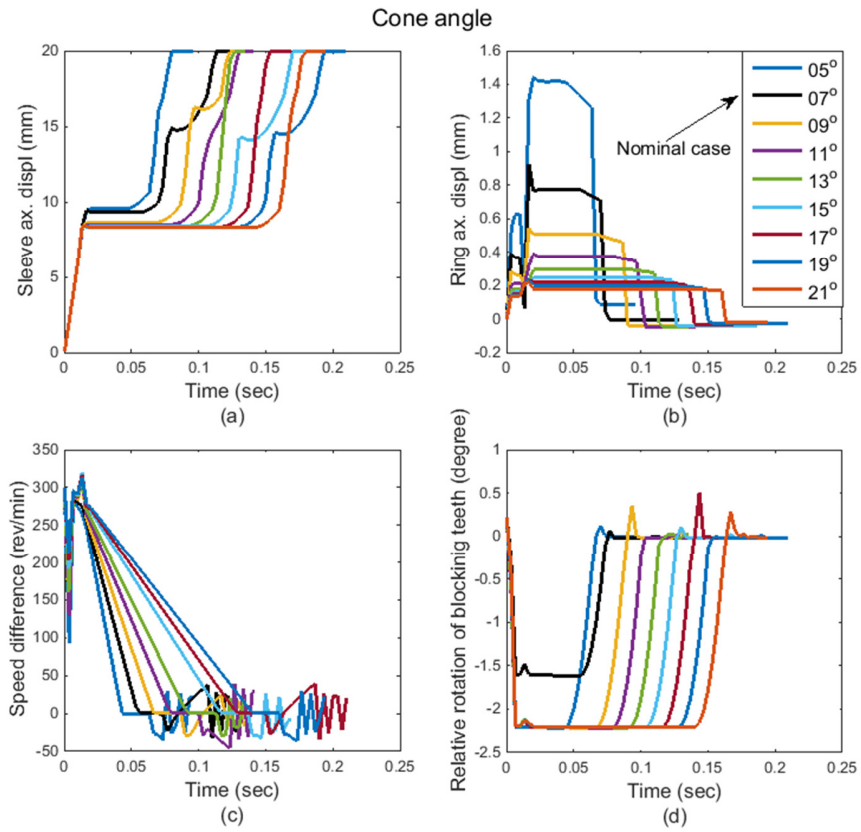Figure 6: Performance monitoring by varying indexing angle.

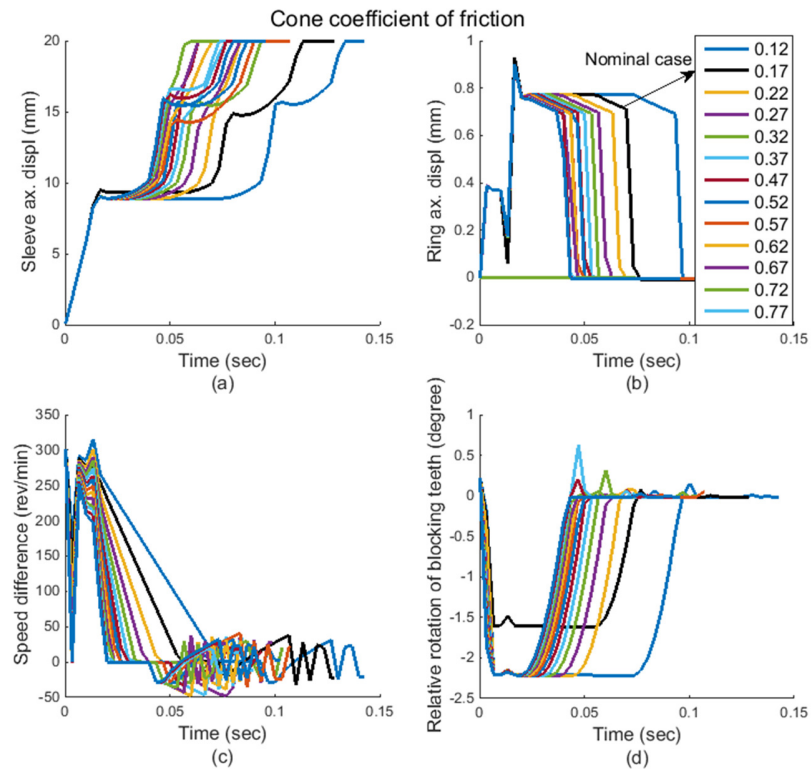Figure 7: Performance monitoring by varying cone angle.

Figure 8: Performance monitoring by varying cone coefficient of friction.

The synchronization time decreases with increasing cone coefficient of friction by monitoring axial displacements of the sleeve and the ring, speed difference and relative rotation of the blocking teeth as shown in Figure 8. For example at 0.17 friction coefficient the ring comes back at its neutral position again at end of the process in shorter time than at 0.12 friction coefficient. With the criterion of failure as a longer synchronization time it can be said the mechanism fails to perform at lower friction coefficient.

Performances of the synchronizer show variation of cone radius can predict the failure mode in terms of the undesirable longer synchronization time. With decreasing cone radius the synchronization time increases. At 80 mm cone radius the ring reaches at its neutral position again at end of the process in shorter time than at 60 mm cone radius as shown in Figure 9. Lowest cone radius can produce failure mode.
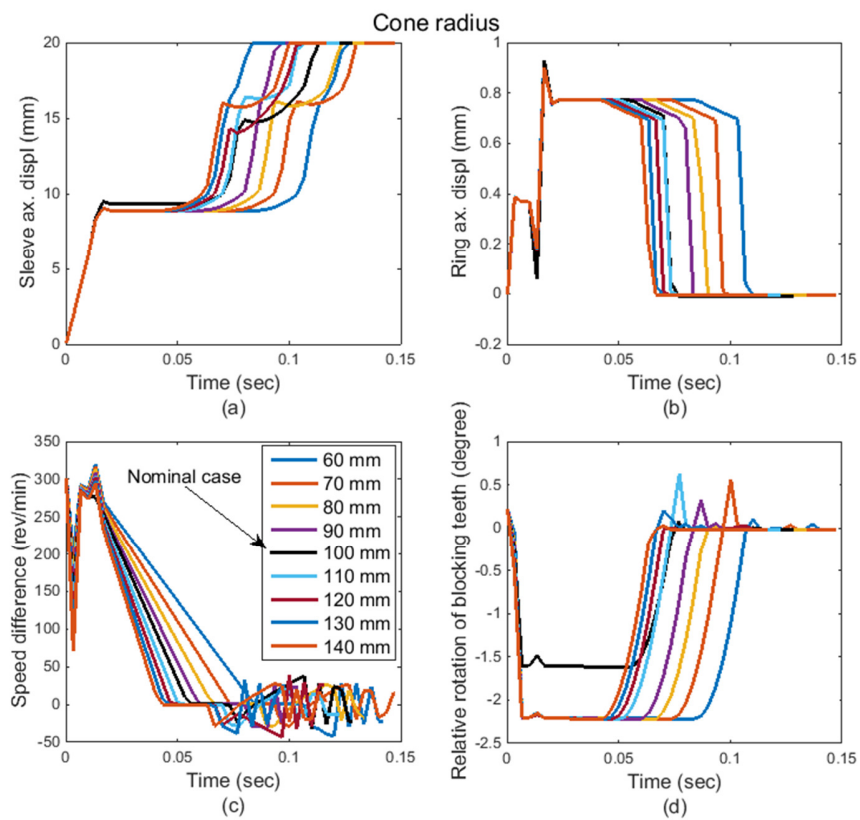

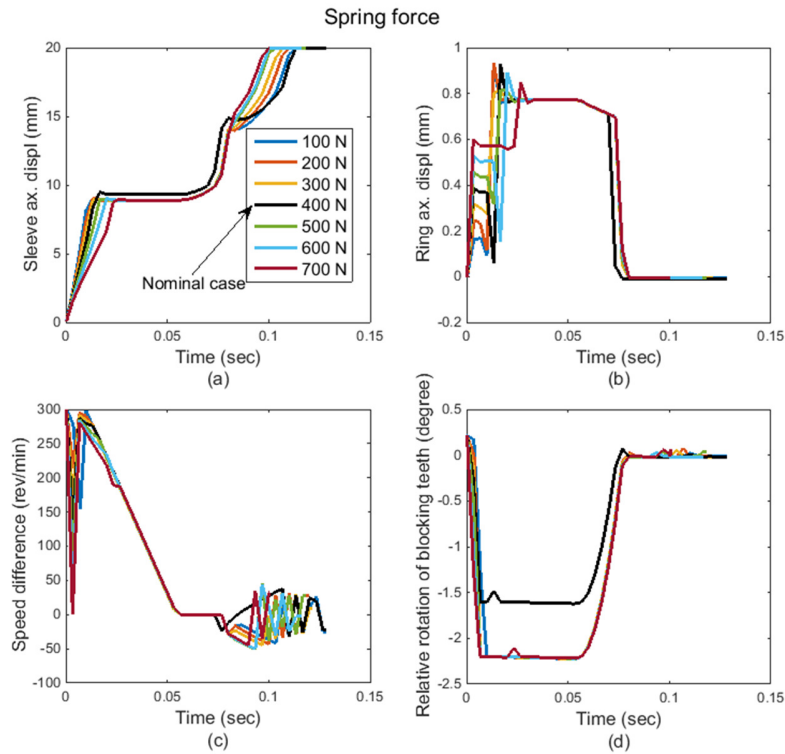Figure 9: Performance monitoring by varying cone radius.

Figure 10: Performance monitoring by varying spring force.

The spring force should not be higher than the shift force otherwise the sleeve will not move axially and the synchronization process cannot start. Less difference between the spring force and the shift force increases the synchronization time as shown in Figure 10. At 700 N spring force the sleeve axial speed is almost similar to the sleeve axial speed at 600 N spring force. Similar phenomenon can be seen from the ring axial displacement and relative rotation of the dog teeth. In case of the spring force failure mode can be predicted in terms of duration of the synchronization time.

Different control design and structural design parameters produce failure modes in different terms of failure. Higher values of the blocker angle and the indexing angle produce failure modes by blocking sleeve of the synchronizer as shown in Figure 5 and 6. Higher values of the shift force produce failure modes in terms of clashing of the engagement teeth as shown in Figure 4. Higher values of the spring force and the cone angle, lower values of the cone coefficient of friction and the cone radius produce failure modes by increasing the synchronization time as shown in Figure 7-9.

Value of the control design parameter and the structural design parameters at which the mechanism produce failure are shown below with the type of failure mode.

$$[\text{mode 1}] = [clashing] = [F_{shf} \geq 2000\ N]$$

To be on safe side 2000 N shift force is taken which produce failure mode.

$$[\text{mode 2}] = [blocking] = \begin{bmatrix} \beta \geq 80^o \\ \delta \geq 7^o \end{bmatrix}$$

13

$$[\text{mode 3}] = [longer\ t_{synch}] = \begin{bmatrix} \alpha > 11^o \\ \mu_\alpha < 0.12 \\ r_\alpha \leq 70\ mm \\ F_{spr} \geq 700\ N \end{bmatrix}$$

To select values of F_{shf} and F_{spr} following condition must be satisfied

$$\left(F_{shf} - F_{spr}\right) \geq 200$$

Synchronization failure modes predictions at lower/higher bounds of the values are given in Table 3.

Besides prediction of the failure modes, a secure prediction in terms of higher or lower limits of values of the control design and the structural design parameters can also be made by sensitivity analysis. Higher values of the cone coefficient of friction and the cone radius and lower values of the shift force, the cone angle and the indexing angle produce optimized performance of the gear shifting mechanism. But in case of the shift force there is transition state between the optimal performance and the failure mode. At which value of the shift force the synchronizer performs optimally, just above that value the synchronizer produces failure mode. Prediction of optimal performances at lower/higher bound are also given in Table 3.

Objective function	No.	Independent variables	Failure mode at lowest/highest bound	Optimal performance at lowest/highest bound
Synchronization time, $\left(t_{synch}\right)$	1	Shift force	Highest	Highest
	2	Blocker angle	Highest	Lowest
	3	Indexing angle	Highest	Lowest
	4	Cone angle	Highest	Lowest
	5	Cone coefficient of friction	Lowest	Highest
	6	Cone radius	No failure/lowest	Highest
	7	Spring force	Near to shift force	lowest

Table 3: Prediction of lower/higher bound of control design and structural design parameters for failure modes and optimal performance.

4   Optimization of the control design and structural design parameters

After identification of the failure modes it is a question of curiosity to find out the optimized control design and structural design parameters values. For optimization the synchronization time is selected as an objective function to be minimized. Advanced direct optimization routine of the GT-Suite model is applied by considering the control design and structural design parameters as independent variables and the synchronization time as a dependent variable. Genetic algorithm is selected as a search method, and the population size and number of generations are selected as a number of 200. In addition to the control design and structural design parameters of the study, rest of the parameters values to run the simulation are chosen as given in Table 1.

Presentation of the results after optimization is not an easy task in case of several input parameters. As the optimization routine tries to find out optimal area from design space of the independent parameters to minimize the synchronization time therefore all of the parameters in design space are plotted. Because of these simple plots it is comparatively easier to find out optimal values of the control design and structural design parameters. Number of iterations, the synchronization time and the control design and structural design parameters are plotted in Figure 11 and 12. Values of the control design and structural design parameters around the more crowded areas in Figure 11 and 12 are selected as optimal values because the GT-Suite model routine finds these crowed areas again and again for the minimum synchronization time during searching of the optimal area from the design space. Approximate values of the control design and structural design parameters around the crowded areas, their percentage change from initial value and lower\upper bounds of the values are given in Table 4.

In Figure 11 the shift force, the indexing angle and the blocking teeth right and left angle are plotted. All four sub Figure 11 (a-d) have two kind of crowded areas; one is with respect to no. of iteration with red color and second is with respect to the synchronization time with black color. In Figure 11 (a) the crowded area is around 2400 N to 2500 N. For the shift force 2500 N is selected as optimized value because it is already found out during prediction of the failure mode that possible highest value of the shift force is desirable for optimal performance. Second cause of selection of 2500 N force is the crowded area of black points of the minimum synchronization time from 0.01 sec to 0.02 sec as shown in Figure 11 (a). In case of the indexing angle there are almost three crowded areas in Figure 11 (b) because lowest indexing angle is predicted as optimal angle during prediction of the failure mode therefore indexing angle at most left crowded area is selected as an optimal value. There are three black points' crowded areas for synchronization time and three of them have no any sufficient difference. So, based upon the crowded area of the no. of iteration and lowest indexing angle from failure mode 4 degree indexing angle is selected as an optimal value. Practically blocker teeth are dealt with two angles; one is right angle and second is left angle. Before in this study for simplicity both angles are considered as same and studied with single value. But for optimization because of unavailability of such kind of simplicity in GT-Suite model the blocking teeth are studied with its two angles. In Figure 11 (c) and (d) both kind of crowded areas with respect to no. of iterations and with respect to the synchronization time are at same position. Based on these positions 50 degree for right angle and 50 degree for left angle of the blocking teeth are selected as optimal values. With similar kind of observations from Figure 12 (a-d) optimal values of the cone angle, the cone coefficient of friction, the cone maximum radius, the cone minimum radius and the spring force are given in Table 4. Initial values, optimized average values, percentage changes and variables bounds for values of the independent variables and the objective function are given in Table 4. In this simplified model of GT-Suite software the spring force is not able to optimize therefore the spring force is not chosen for further study.
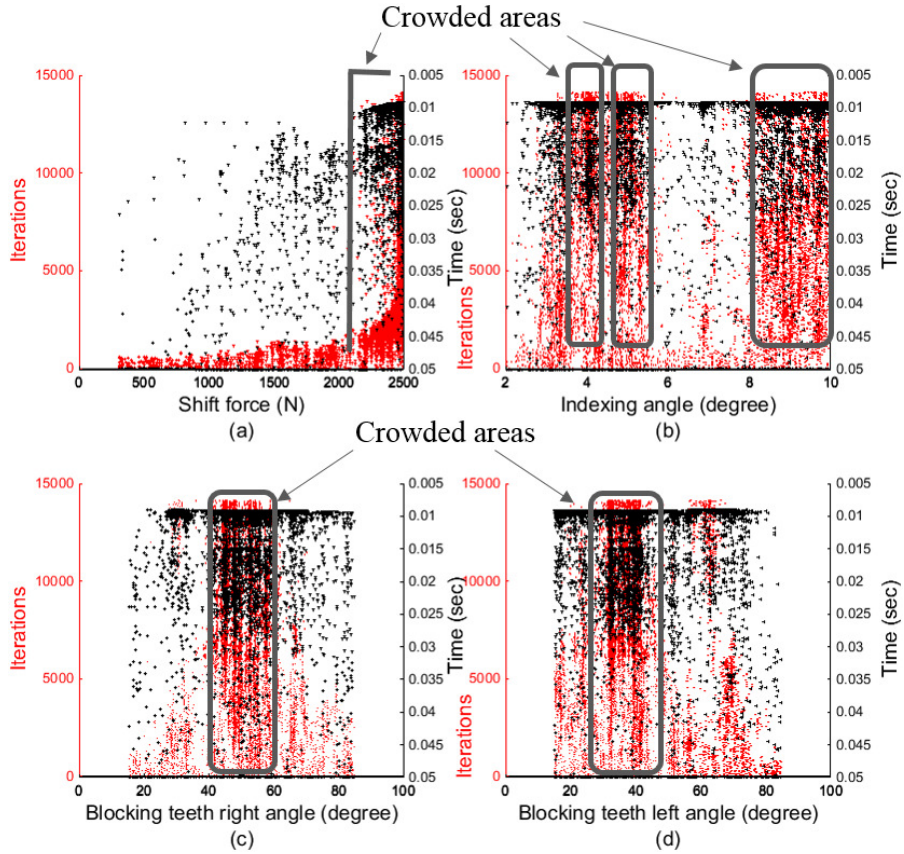
Figure 11: Correlation of optimized synchronization time and no. of iterations with control design and structural design parameters.
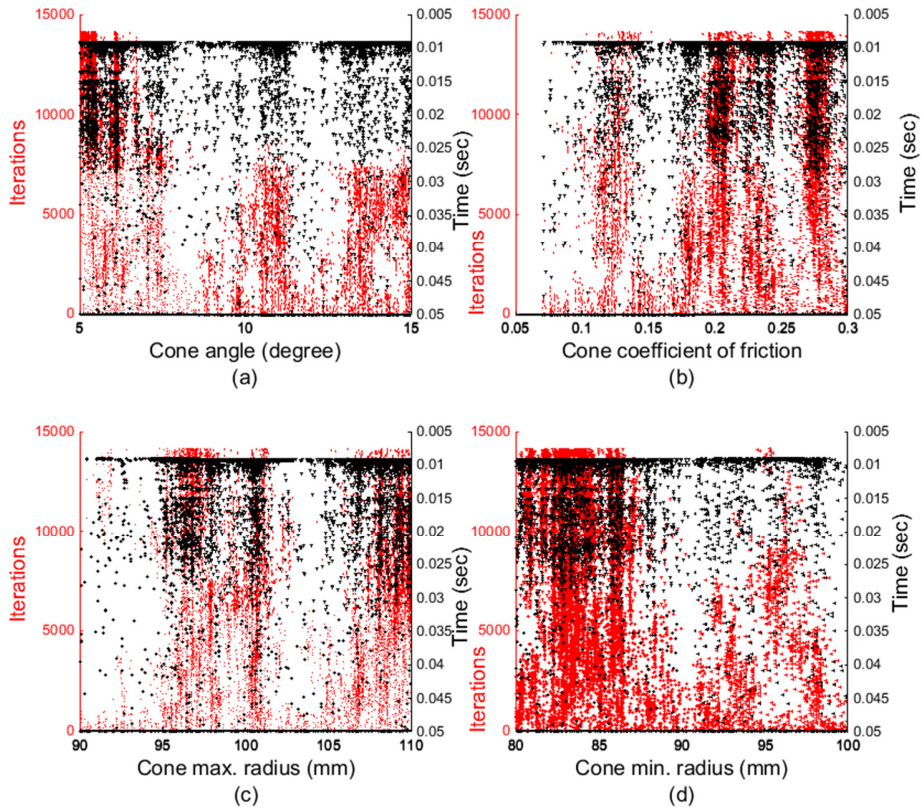

Figure 12: Correlation of optimized synchronization time and no. of iterations with the structural design parameters.

Objective function		No.	Independent variables	Initial values	Variables bounds	Optimized average values	Percentage change
Synchronization time (t_{synch}) (sec)		1	Shift force (N)	1000	300-2500	2500	150
		2	Indexing angle	4.6	2-10	4	13.0
Initial value	Optimized value	3	Blocking teeth right angle	57.7	15-85	45	22
0.118	0.009	4	Blocking teeth left angle	50	15-85	35	30
Percentage change		5	Cone angle (deg)	7	5-15	5	28.6
92		6	Cone coefficient of friction	0.17	0.07-0.3	0.27	58.8
		7	Cone max. radius	100.75	90-110	110	09
		8	Cone min. radius	99.25	80-100	83	16.4

Table 4: Percentage change of input parameters after optimization.

5   Analysis of the synchronizer performance at optimized parameters values

The performance diagram at optimized values of the control design parameter and the structural design parameters is shown in Figure 13. This is the ideal performance of the gear shifting mechanism where it can be seen that the sleeve moves axially without any interruption. But rotational speed of the gear does not increase till near to end of the process and suddenly the gear gains rotational speed drastically. Even the gear crosses 1000 rpm which is speed of the sleeve and approaches more than 1200 rpm. But this ideal performance could be practically not possible. So performance diagram shown in Figure 14 is plotted at optimized values of the parameters except the shift force. Instead of the optimized value, 2500 N the shift force of 1250 N is applied. It can be seen from the Figure 14 that rotational speed of the gear seems to be practical. But the synchronization time with 2500 N shift force is 0.01 sec and with 1250 N is 0.036 sec. Still the synchronization time at 1250 N shift force is less than the synchronization time at nominal values which is 0.1 sec.

At iteration number 14019 values of the optimized parameters are

$$
\begin{bmatrix}
F_{shf} \\
\beta_{rgt} \\
\beta_{lft} \\
\delta \\
\alpha \\
\mu_{\alpha} \\
r_{\alpha,max} \\
r_{\alpha,min}
\end{bmatrix}
= [2497.9 \quad 3.9 \quad 45 \quad 34 \quad 5 \quad 0.3 \quad 97 \quad 82]^{T}
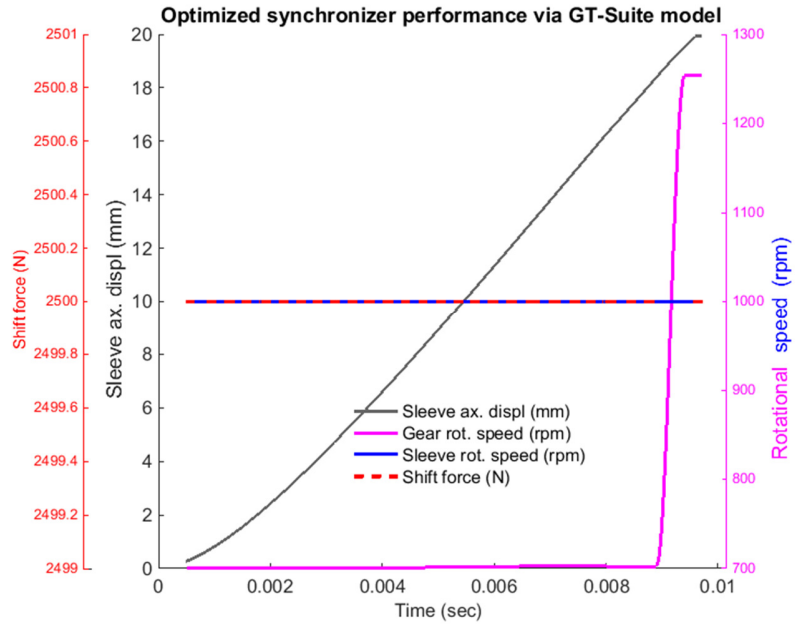$$

17

Figure 13: Performance of the gear shifting mechanism at optimized values of the parameters.
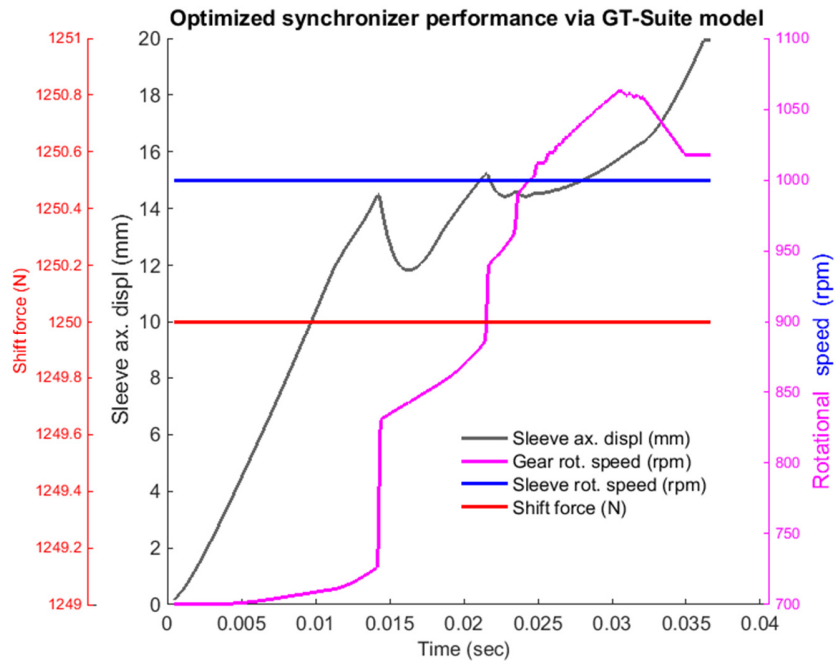

Figure 14: Performance of the gear shifting mechanism at optimized values of the parameters except shift force.

18

6 Optimization of the structural design parameters by GT-Suite model

As it is observed in optimization results that the control design parameter can be excluded from the optimization process and still optimized performance of the gear shifting mechanism can be obtained by optimizing only structural design parameters. So, in this section the structural design parameters are optimized by using the GT-Suite software at 1000 N, 1250 N, 1500 N, 1750 N and 2000 N shift forces. Values of the optimized parameters obtained after optimization are shown in Table 5. The synchronizer performance diagram at 1000 N and 1250 N shift force with corresponding to optimized values of the structural design parameters are shown in Figure 15 and Figure 16. Although the optimized values of the structural design parameters are different at different shift forces but performances of the mechanism are almost similar. t_{synch} at 1000 N, 1250 N, 1500N and 2000 N is almost same which is 0.03 sec and performance diagrams at 1000N and 1250 N are almost similar. Even optimized values of the structural design parameters at different values of the shift forces vary within a short range. For example indexing angle varies between 3° and 5°, cone coefficient of friction varies between 0.27 and 0.3, cone maximum radius varies between 105 mm and 110 mm, cone minimum radius varies between 82 mm and 91 mm, cone angle varies between 8° and 12°, blocker teeth right angle varies between 45° and 50° and blocking teeth left angle varies between 43° and 54°. Under this scenario it is concluded that with minimum shift force and optimized structural design parameters optimized performance of the gear shifting mechanism can be obtained.

Independent variables	Optimized results at F_{shf_o} = 1000 N	Optimized results at F_{shf} = 1250 N	Optimized results at F_{shf} = 1500 N	Optimized results at F_{shf} = 1750 N	Optimized results at F_{shf} = 2000 N	Optimized results at F_{shf} = 2500 N
Indexing angle (deg)	4	3	4	5	4	3.5
Blocking teeth right angle (deg)	45	50	50	48	50	45
Blocking teeth left angle (deg)	43	40	50	46	40	54
Cone angle (deg)	12	10	12	8	12	12
Cone coefficient of friction	0.27	0.27	0.27	0.24	0.27	0.3
Cone max. radius (mm)	110	105	105	105	107	105
Cone min. radius (mm)	83	88	88	85	82	91
Synchronization time t_{synch} (sec)	0.03	0.03	0.03	0.03	0.02	0.009

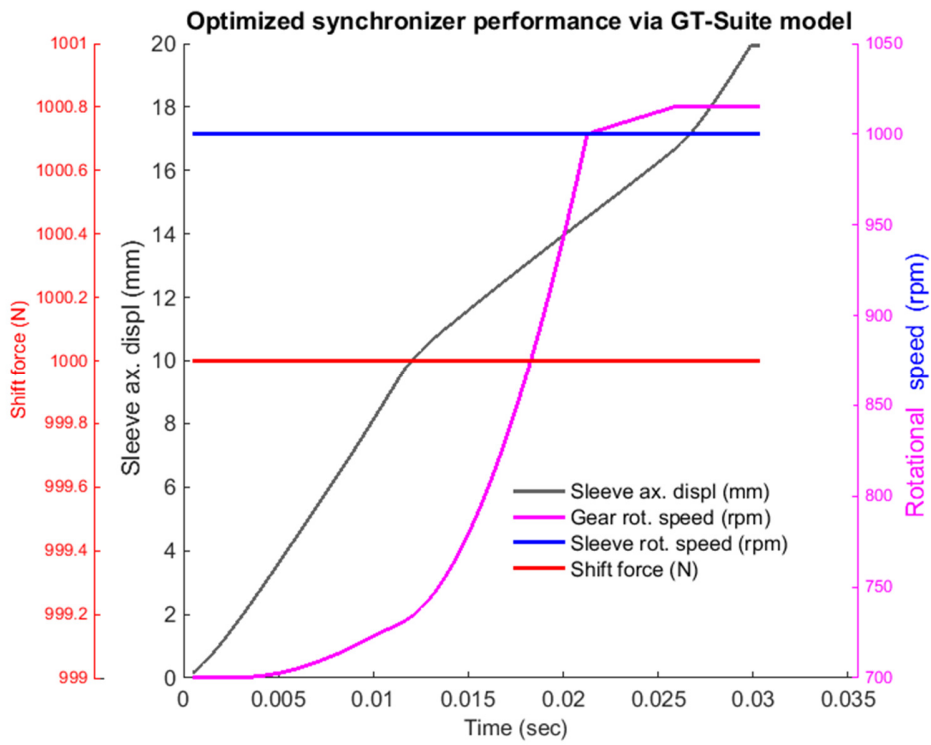Table 5: Results of optimization of the structural design parameters.

Figure 15: Performance of the gear shifting mechanism at optimized values of the parameters for shift force = 1000N.
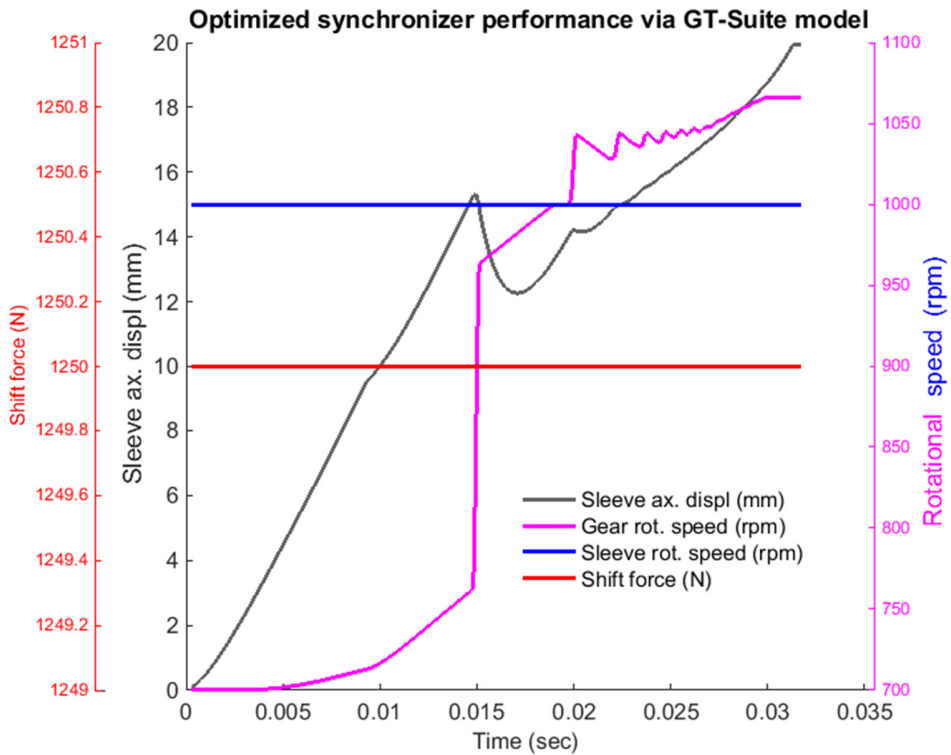

Figure 16: Performance of the gear shifting mechanism at optimized values of the parameters for shift force = 1250N.

7 Conclusions

A contribution is made to improve performance of the gear shifting mechanism. Limits of values of the control design and structural design parameters are identified at which the synchronizer fails to perform by using the developed GT-Suite model of a gear shifting mechanism. Shift force as the control design parameter and blocking angle, indexing angle, cone angle, cone coefficient of friction, cone radius and spring force are selected as the structural design parameters. Sleeve and ring axial displacements, speed difference and relative rotation of the blocking teeth are chosen to monitor performance of the synchronizer for identification of the failure modes. It is concluded that variations of the shift force predict the failure modes in terms of clashing. Variations of the blocker angle and the indexing angle predict failure modes in terms of blockage of the sleeve. Variations of the cone angle, the cone coefficient of friction, the cone radius and the spring force predict failure modes in terms of the longer synchronization time. Generally the synchronizer fails to perform at lower values of the cone radius and the cone coefficient of friction and at higher values of the shift force, the cone angle, the blocker angle, the indexing angle and the spring force.

Optimization routine of GT-Suite model is applied with the genetic algorithm to identify values limits of the control design and structural design parameters at which the synchronizer can perform optimally. Reasonable bounds of the parameters are implemented with initial values to run the optimization routine of the GT-Suite model. The control design and structural design parameters are considered as independent parameters and the synchronization time is considered as an objective function to be minimized. The control design and structural design parameters are plotted against no. of iterations and the synchronization time to draw valuable conclusions from Figure 11 and Figure 12. From crowded areas of points it is concluded generally that at lower values of the shift force, the cone angle, the cone radius and the cone coefficient of friction and at higher values of the blocker angle, the indexing angle and the spring force, the synchronizer perform optimally in sense of minimum value of synchronization time. Analyses of performance of the gear shifting mechanism at optimized values of the parameters depicted in Figure 13 shows that it could not be possible practically to achieve such a less synchronization time because the gear drastically gains rotational speed almost near to end of the process. Later on number of optimizations are performed at different particular values of the shift force (1000 N, 1250 N, 1500 N, 1750 and 2000 N) to obtain the optimized structural design parameters. It is found that optimized performance of the gear shifting mechanism can be obtained at lower value of the shift force by using optimized values of the structural design parameters. In addition to this difference in t_{synch} between the higher shift force and lower shift force is not so big, at 2500 N t_{synch} is 0.009 sec and at 1000 N t_{synch} is 0.03 sec but at nominal values of the structural design parameters t_{synch} is 0.118 sec. So it is concluded that lower shift force, 1000 N and optimized structural design parameters in this study can be used to get minimum synchronization time.

The gear shifting mechanism has more than studied the control design and structural design parameters which cannot be ignored to approach the practical optimal performance which may be studied in future. The GT-Suite model needs to be updated towards the real application for identification of the failure modes.

Acknowledgements

References

[1] D. Häggström, U. Sellgren, W. Stenström and S. Björklund , ”A Verified and Validated Model for Simulation-Driven Design of Heavy Duty Truck Synchronizers,” in *ASME 2015 Power Transmission and Gearing Conference; 23rd Reliability, Stress Analysis, and Failure Prevention Conference*, Boston, Massachusetts, August 2–5, 2015.

[2] D. Häggström, W. Stenström and S. Björklund, "*Evaluation of synchronizer loading parameters and their ability to predict failure,*" Proceedings of the Institution of Mechanical Engineers, Part J: Journal of Engineering Tribology, October 31, 2017.

[3] H. Szöky J. Murin and V. Goga, "Failure of Synchronization in A Manual Gearbox," *Journal of Engineering,* vol. 04, no. 10, pp. 25-30, 2014.

[4] G. Bóka, J. Márialigeti et al., "Face dog clutch engagement at low mismatch speed," Periodica Polytechnica Transportation Engineering, [S.l.], v. 38, n. 1, p. 29-35, 2010. ISSN 1587-3811.

[5] L. Lovas, "Etude des relations entre le comportement et la fabrication des synchronisateurs des synchronisateurs des," National Institute of Applied Sciences, Lyon, PhD Thesis, 2004.

[6] M. Irfan, V. Berbyuk and H. Johansson, "Constrained Lagrangian Formulation for modelling and analysis of transmission synchronizers," 2015:05 Department of Applied Mechanics Chalmers University of Technology, Gothenburg, 2015.

[7] M. Irfan, V. Berbyuk and H. Johansson, "Modelling of Heavy Vehicle Transmission Synchronizer using Constrained Lagrangian Formalism," in *International Conference on Engineering Vibration*, Ljubljana, Slovenia, 7-10 September 2015.

[8] M. Irfan, V. Berbyuk and H. Johansson, "Dynamics and Pareto Optimization of a Generic Synchronizer Mechanism," in *Rotating Machinery,* Proceedings of the 34th IMAC, *A Conference and Exposition on Structural Dynamics*, *Volume 8, pp. 417-425,* http://dx.doi.org/10.1007/978-3-319-30084-9_38, 2016.

[9] M. Irfan, Modelling and optimization of gear shifting mechanism, Application to heavy vehicles transmission systems. 2017:01 Department of Applied Mechanics, Chalmers University of Technology, Gothenburg, 2017.

[10] M. Irfan, V. Berbyuk and H. Johansson, *Performance control of the transmission synchronizer via sensitivity analysis and parametric optimization,* journal of Cogent Engineering, 2018. (submitted).

[11] V. Berbyuk, "Towards pareto optimization of performance of a generic synchronizer of transmission systems," in *In proceedings of IDETC/CIE 2015 ASME Conference*, Boston, USA, August 2-5, 2015 paper DETC 2015-46773. http://dx.doi.org/10.1115/DETC2015-46773.

[12] M. Irfan, V. Berbyuk and H. Johansson, "Verification of the Transmission Synchronizer Model," in *Svenska Mekanikdagarna*, Uppsala, Sweden, p. 48. 12-13 June 2017.

[13] Fresh Design Studio, "GT-SUITE," Gamma Technologies LLC, [Online]. Available: https://www.gtisoft.com/. [Accessed 2015-2017].